Stability Analysis of Large-Scale Incompressible Flow Calculations on Massively Parallel Computers

Andrew G. Salinger, Richard Lehoucq, and Louis Romero

Sandia National Laboratories[1]
Albuquerque, NM 87185-1111, USA

ABSTRACT

A set of linear and nonlinear stability analysis tools have been developed to analyze steady state incompressible flows in 3D geometries. The algorithms have been implemented to be scalable to hundreds of parallel processors. The linear stability of steady state flows are determined by calculating the rightmost eigenvalues of the associated generalize eigenvalue problem. Nonlinear stability is studied by bifurcation analysis techniques. The boundaries between desirable and undesirable operating conditions are determined for buoyant flow in the rotating disk CVD reactor.

INTRODUCTION

With modern algorithms and parallel computers, incompressible flow models on complex three-dimensional (3D) geometries can be solved quickly and reliably. When a fully-coupled Newton method is used [1], coupled with a scalable iterative linear solver, it is possible to directly calculate steady-state solutions. We have previously used such algorithms to study the chemical vapor deposition of Gallium Arsenide, where parameters studies consisting of dozens of steady-state calculations were used to suggest design modifications [2-5].

Steady-state algorithms, as opposed to transient algorithms, converge indiscriminately to stable and unstable solutions. One way to determine the linear stability of a steady state solution is to linearize the problem about the solution and then solve the associated generalized eigenvalue problem. If all the eigenvalues have negative real part, than small disturbances decay in time; however, any eigenvalues with positive real parts imply that the solution is unstable because any disturbances aligned with the associated eigenvectors will grow. The Cayley transformation, coupled with a robust eigen-solver, can be used to identify several rightmost eigenvalues. This methodology has been used successfully by a few groups [6-9].

The linear stability analysis can only determine local stability; complementary nonlinear analysis techniques can be used to probe the global behavior. Bifurcation analysis techniques such as continuation methods [10] can locate such phenomena as turning points and regions of parameter space that exhibit multiple steady state solutions [11].

In this paper, we demonstrate how augmenting a robust steady-state flow code with a set of stability analysis algorithms can yield a powerful tool for analyzing engineering flow problems. In addition, we show that careful implementation of these tools can lead to algorithms that scale to hundreds of parallel processors and models consisting of millions of unknowns.

1. This work was partially funded by the United States Department of Energy, Mathematical, Information, and Computational Sciences Division under contract no. DE-AC04-94AL85000. Sandia is a multiprogram laboratory operated by Sandia Corporation, a Lockheed Martin Company, for the United States Department of Energy.

NUMERICAL METHODS: Eigensolver

The algorithms and parallel implementation of the linear stability analysis algorithms has been detailed in a previous report [8]. After a steady-state solution to the incompressible Navier-Stokes equations are calculated, the evolution equations are linearized about the steady state. The associated generalized eigenvalue problem has the form

$$\mathbf{J}z = \lambda \mathbf{M}z, \qquad (1)$$

where $\mathbf{J}$ is the Jacobian matrix, $\mathbf{M}$ is the mass matrix, z is an eigenvector, and λ its associated eigenvector. A Cayley transformation, which includes two adjustable real parameters, σ and μ, is used to reformulate the generalized eigenvalue problem into an ordinary eigenvalue problem for the transformed eigenvalues γ:

$$(\mathbf{J} - \sigma\mathbf{M})^{-1}(\mathbf{J} - \mu\mathbf{M})z = \gamma z. \qquad (2)$$

A simple relationship exists between the transformed and original eigenvalues,

$$\gamma = \frac{\lambda - \mu}{\lambda - \sigma}. \qquad (3)$$

Appropriate choices of σ and μ are made so that the eigenvalues of interest (those λ with largest real part) are mapped to the eigenvalues of largest magnitude in the Cayley system.

The eigenvalue problem defined in equation (2) is solved using Arnoldi's method using a version of the P_ARPACK software [12,13] modified to perform the Cayley transformation. With proper choices of σ and μ, we found that an Arnoldi spaces of size 24 was typically sufficient for calculating eigenvalues to three digits of accuracy. The main hurdle for a scalable algorithm is the solution of the linear set of equations (2) to sufficient accurcay with an parallel iterative matrix solver. Details can be found in a previous paper [8].

NUMERICAL METHODS: Bifurcation Analysis Algorithms

The nonlinear analysis algorithms are used to detect and delineate regions of multiple steady states. The two algorithms used in this work are a pseudo arc-length continuation algorithm and a turning point (a.k.a. saddle point) bifurcation tracking algorithm. Each of the algorithms was implemented using bordering algorithms, which require minimal intrusiveness to the code that was already set up to do a fully coupled Newton method. Routines where written that have just three main calls to the MPSalsa finite element code: (1) Calculate a residual vector given a solution vector and a parameter value; (2) Calculate a Jacobian matrix given a solution vector and a parameter value; and (3) Solve a linear system given a Jacobian matrix and right hand side. Since the linear systems all involve the same Jacobian matrix as solved by the steady-state code, these algorithms do not require modification of the matrix fill routine, sparse matrix allocation, or parallel communication maps.

The pseudo arc-length continuation algorithm [10] allows steady-state solution branches to be tracked around turning points, by basing the continuation algorithm on a monotonic arc-length variable s in place of the system parameter p. This requires a modification to the Newton algorithm. The usual Newton iteration for reaching a steady-state solution vector x is to solve

$$R(x, p) = 0 \quad \text{with Newton iteration}$$
$$\mathbf{J}\delta x = -R, \qquad (4)$$

where R is the residual equations from the PDE discretization, $\mathbf{J}$ is the Jacobian matrix, and δx is the update to the latest estimate of the solution vector. For arc-length continuation, an additional constraint equation N, which ensures that the next solution is a distance s from the previous solution, is solved simultaneously with the steady-state equations. Newton's method on this augmented nonlinear system is used to solve for unknowns x and p, and has the form,

$$\begin{aligned} R &= 0 \\ N(x, p, s) &= 0 \end{aligned} \quad \text{with Newton iteration}$$
$$\begin{bmatrix} J & R_p \\ N_x & N_p \end{bmatrix} \begin{bmatrix} \delta x \\ \delta p \end{bmatrix} = \begin{bmatrix} -R \\ -N \end{bmatrix}. \qquad (5)$$

A bordering algorithm is used to manipulate the Newton iteration so that it requires two linear solves of the matrix $\mathbf{J}$ in place of one solve of the augmented matrix in eq. (5). This does not save CPU times but leads to much easier implementation within a code that is already set up for solving sets of linear equations coming from the Jacobian matrix.

Solution branches can pass through turning points. These bifurcations signify the creation or destruction of two steady state solution branches and can delineate regions of multiplicity. In our example problem in the next section, the turning point is also the global stability limit for the desirable flow pattern. At a turning point one eigenvalue of the matrix is identically zero, and we use this fact to directly calculate the bifurcation. For small systems of equations, this can be specified with a single additional constraint equation, that the determinant of the Jacobian matrix is zero. However this is not a feasible calculation for large systems of equations. We use the fact that there exists a null vector n (the eigenvector associated with the zero eigenvalue) of unit length in the null space of $\mathbf{J}$. This leads to a system of system of $2N_x + 1$ equations and unknowns (x, n, and p), where N_x is the length of x (and the order of $\mathbf{J}$),

$$\begin{aligned} R &= 0 \\ \mathbf{J}n &= 0 \quad \text{with Newton iteration} \\ l^t n &= 1 \end{aligned}$$
$$\begin{bmatrix} \mathbf{J} & 0 & R_p \\ \mathbf{J}_x n & \mathbf{J} & \mathbf{J}_p n \\ 0 & l^t & 0 \end{bmatrix} \begin{bmatrix} \delta x \\ \delta n \\ \delta p \end{bmatrix} = \begin{bmatrix} -R \\ -\mathbf{J}n \\ 1 - l^t n \end{bmatrix}. \qquad (6)$$

The third equation, $l^t n = 1$, is used to set the length of n, which is otherwise arbitrary up to a constant. The form of l^t, often chosen to be the vector of all 1's, can be chosen by the user.

Another bordering algorithm is used to solve the Newton step by requiring only linear solves with the matrix $\mathbf{J}$. This requires four linear solves per Newton step of the augmented. The fact that it is the same matrix each time can be used to save on operations by reusing the preconditioner.

RESULTS

The impact of combining a robust steady-state flow code with linear and nonlinear stability analysis tools is demonstrated on an industrially relevant problem: flow in the rotating disk CVD reactor. This reactor configuration as shown in Figure 1 is commonly used to grow semiconductors such

as gallium arsenide and gallium nitride.

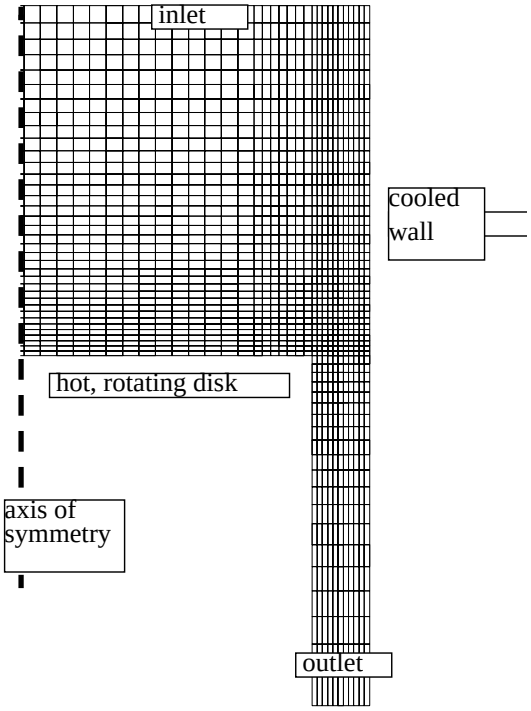

FIGURE 1. Geometry and sample mesh for the axisymmetric model of the rotating disk reactor.

Under ideal circumstances, the flow patterns approach those of the von Karman similarity solution [14]. This leads to very uniform film growth rates across the susceptor which in turn can lead to high quality films. However, it has been shown experimentally and numerically that undesirable flow patterns can occur [15-17] due to the destabilizing buoyancy force of the fluid being heated from below.

Our model involves the incompressible Navier-Stokes equations, the continuity equation, and a heat balance. In this paper we use the Boussinesq approximation for modelling buoyancy and fix all physical properties constant. Although the temperature differences in this reactor generally warrant temperature dependent properties and in particular an idea gas treatment of density variation with temperature, the simpler model improves the chances of discovering simple scaling laws in the results. In this work, the Prandlt number and the reactor aspect ratio were fixed at unity. The inlet plug flow velocity is fixed at the matching conditions, which is the rate at which an infinite disk would pump in the flow [15]. The other parameters that are varied in this study are the rotational Reynolds number and the Rayleigh number, defined as:

$$Re = \frac{\Omega R^2}{\nu} \quad \text{and} \quad Ra = \frac{g\beta\Delta T \nu^{1/2}}{\Omega^{3/2}\alpha}. \quad (7)$$

In these definitions, Ω in the disk rotation rate, R is the disk radius, ν is the kinematic viscosity, $g\beta\Delta T$ is the gravity magnitude times the thermal expansion coefficient times the temperature difference over the reactor, and α is the thermal diffusivity. In the Rayleigh number there are three length scales in the numerator: in our definition, these are chosen to be the momentum boundary layer thickness, $\sqrt{\frac{\nu}{\Omega}}$. Using an axisymmetric model, we tracked the steady state solutions and located regions where multiple steady states coexist. Figure 2 clearly . shows this region in a plot of the Nusselt number (a measure of heat flux) at the center of the rotating disk as a function of the Rayleigh number (a measure of the buoyancy force). Solution branches labeled A, B, and C exist at the exact same conditions. It was determined through linear stability analysis that solution branch B is unstable, while A and C are stable. By visualizing the solutions it is evident that solutions on branch A exhibit desirable flow pattern similar to the von Karman similarity solution, while solutions on branch C exhibit a buoyancy-induced torroidal recirculation cell.

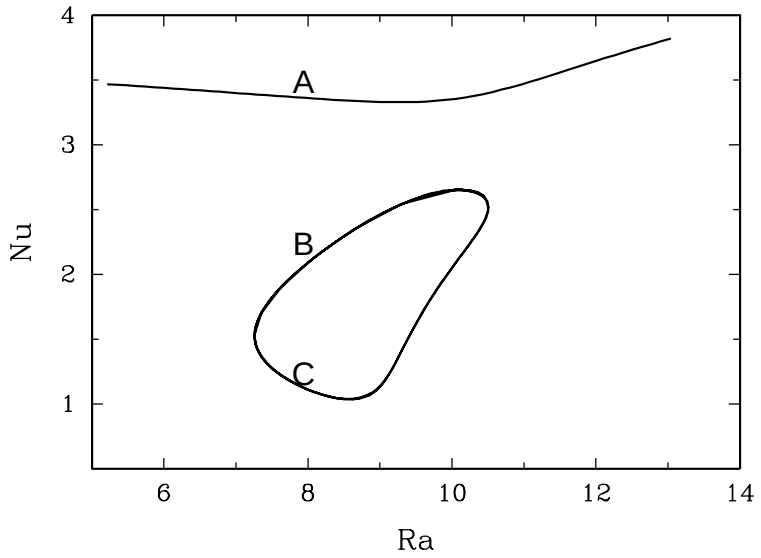

FIGURE 2. Locus of steady state solutions as measured by the Nusselt number at the center of the disk, as a function of the Rayleigh number. The rotational rate is Re=83.4 and the inlet flow rate is at matching conditions. A region of multiplicity is evident.

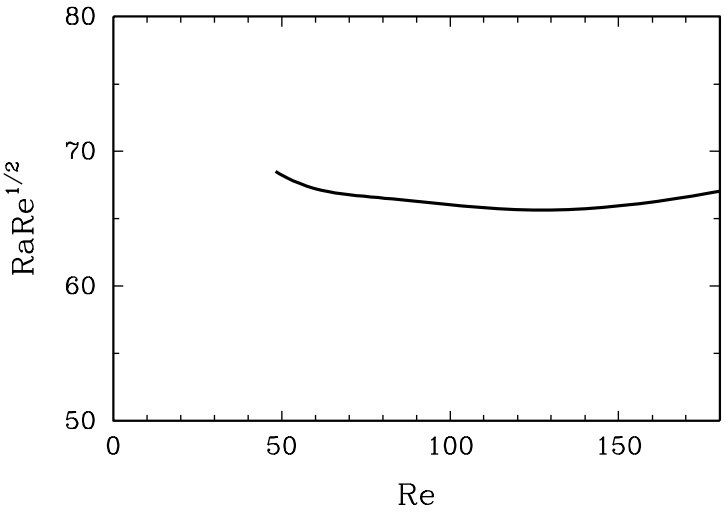

FIGURE 3. Locus of turning points marking the left end of branch C in Figure 2, as a function of the rotational Reynolds number. Designing a reactor to operate below this curve will avoid the chance of seeing the undesirable recirculations of branch C.

While operating on branch A is possible for $Ra > 7$, it is also possible that the reactor would get attracted to branch C. The behavior is dependent on the initial configuration of the reactor, the procedure bringing the reactor to the final conditions, and upon random disturbances. However, if the reactor is designed and operated at $Ra < 7$ where branch C no longer exists, and if our assumption is true that no other solution branches exist at these parameter values, than the reactor must operate at the desirable conditions associated with branch A.

It is therefore necessary only to know the location of the left end of branch C to tell designers how to avoid the reactor operating with these undesirable recirculations. This point is a turning point, and can be converged to with the robustness of Newton's method using the algorithms described above. We have calculated this turning point and then tracked it as a function of the rotational Reynolds number of the reactor, as presented in Figure 3. For the range of Reynolds numbers studied, it appears that a safe reactor design would satisfy the criterion,

$$Ra\sqrt{Re} < 65 \qquad (8)$$

The turning point ends near $Re = 48$, below which there is continuous transition from the desirable to the undesirable flow patterns. Future results will study how this scaling law persists to higher Reynolds numbers and for different reactor aspect ratios.

In addition to knowing the limit of the global stability of the solution branch A, it is also important to know the limits of its local stability. In order to scale-up the reactor to larger deposition surfaces, it might not be feasible to keep within the criterion defined by eq. (8). Also, through careful procedures or sophisticated controls, it might be possible to avoid other stable solution branches.

The determination of local stability limit of this branch should include non-axisymmetric disturbances, so we have studied a full three-dimensional model. The geometry is exactly the same as the axisymmetric model above, but now consists of 500,000 total unknowns and uses an unstructured finite element mesh. This problem was run on 256 processors of the Sandia/Intel Tflop computer, each of which is a 333 MHz Pentium Chip. A single eigenvalue calculation required about 20 minutes to calculate the several largest eigenvalues to sufficient accuracy. A continuation run along solution branch A of Figure 2 was performed, and at each step the rightmost eigenvalues were computed using the algorithms described above. The first two complex pairs of eigenvalues to cross into the positive real plane are plotted as a function of Rayleigh number in Figure 4.

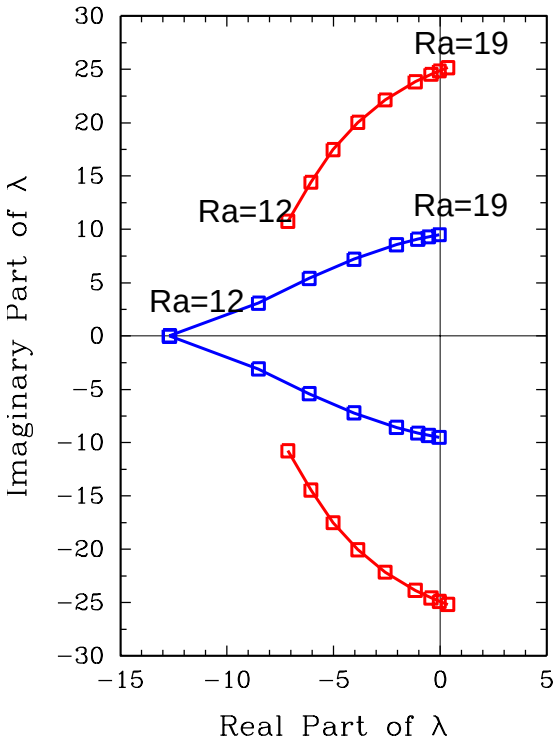

FIGURE 4. Plot of the four largest eigenvalues in the complex plane as a function of the Rayleigh number, along solution branch A in Figure 2, using a 3D model of 500,000 unknowns, The region of linear stability of this branch ends in a Hopf bifurcation near $Ra = 18.5$.

It can be seen that this solution branch loses linear stability to a Hopf bifurcation near $Ra = 18.5$ and is quickly followed by a second Hopf bifurcation near $Ra = 19.0$. This instability represents a hard upper limit for operating this reactor under desirable flow situations, for all other parameters being fixed. Visualization

of the eigenvectors associated with the destabilizing bifurcations revealed that the first bifurcation is an axisymmetric bifurcation. This can be efficiently detected with the axisymmetric model. The second Hopf bifurcation is a mode-1 instability. and this is quickly followed by a third to a mode-2 instability. The proximity of three Hopf bifurcations suggest a region of very complicated dynamics. A mesh convergence study with up to four million unknowns, presented in [7], confirms these results.

CONCLUSIONS

Linear stability and bifurcation analysis routines have been linked to a steady-state, finite element, parallel, incompressible flow code. The power of these tools is demonstrated on a significant engineering design problem: avoiding recirculating flows in the rotating disk chemical vapor deposition reactor. A region of solution multiplicity is determined using arc-length continuation. For a region of two-parameter design space, a simple design rule for avoiding the possibility of simple torroidal recirculations is proposed, based on the direct calculation of the turning point where this undesirable flow pattern originates. Using a scalable eigenvalue calculation routine applied to a 3D flow model, the value of one key design parameter is determined which corresponds to the loss of the local stability of the desirable flow branch.

REFERENCES

1. J.N. Shadid, R.S. Tuminaro and H.F. Walker, “An Inexact Newton Method for Fully Coupled Solution of the Navier-Stokes Equations with Heat and Mass Transport,” *JCP,* 137 (1997) 155-185;
2. J. N. Shadid, H. K. Moffat, S. A. Hutchinson, G. L. Hennigan, K. D. Devine, and A. G. Salinger, “MPSalsa: a finite element computer program for reacting flow problems part 1 - theoretical development,” *Sandia National Laboratories Technical Report,* SAND95–2752 (1996).
3. A.G. Salinger, K.D. Devine, G.L. Hennigan, H.K. Moffat, S.A. Hutchinson, and J.N. Shadid, MPSalsa: a finite element computer program for reacting flow problems part 2 - user’s guide,” *Sandia National Laboratories Technical Report,* SAND96-2331 (1996).
4. S. A. Hutchinson, J. N. Shadid and R. S. Tuminaro, “Aztec User’s Guide: Version 1.0,” *Sandia National Laboratories Technical Report,* SAND95–1559 (1995).
5. A.G. Salinger, J.N. Shadid, S.A. Hutchinson, G.L. Hennigan, K.D. Devine, H.K. Moffat, “Analysis of gallium arsenide deposition in a horizontal CVD reactor using massively parallel computations,” *J. Crystal Growth* 203 (1999) 516-533.
6. K. A. Cliffe, T. J. Garratt and A. Spence, “Eigenvalues of the discretized Navier-Stokes equation with application to the detection of Hopf bifurcations,” *Advances in Computational Mathematics,* 1 (1993) 337-356.
7. R.B. Lehoucq and A.G. Salinger, “Massively parallel linear stability analysis with P_ARPACK for 3D fluid flow modeled with MPSalsa,” *Applied Parallel Computing, PARA’98,* B. Agstrom, Dongarra, J., Elmroth, E. and Wasniewski, J., Editors, *Lecture Notes in Computer Science*, No. 1541, Springer-Verlag (1998) 286-295.
8. R.B. Lehoucq and A.G. Salinger, “Large-scale eigenvalue calculations for

stability analysis of steady flows on massively parallel computers," submitted to *Int'l J. Numerical Methods in Fluids*, (1999).

9. M. Morzynski, K. Afanasiev, and F. Thiele, "Solution of the eigenvalue problem resulting from global non-parallel flow stability analysis," *Computer Methods in Applied Mechanics and Engineering*, 169 (1999) 161-176.

10. H.B. Keller, in *Applications of Bifurcation Theory*, P.H. Rabinowitz editor, Academic, New York, (1997), 359.

11. A.G. Salinger, S. Brandon, R. Aris, and J.J. Derby, "Buoyancy driven flows of a radiatively participating fluid in a vertical cylinder heated from below," *Proc. Royal Soc. A*, 442 (1993) 313-341.

12. R. B. Lehoucq, D. C. Sorensen and C. Yang, *ARPACK USERS GUIDE: Solution of Large Scale Eigenvalue Problems with Implicitly Restarted Arnoldi Methods*, SIAM press (1998), Philadelphia, PA.

13. K. J. Maschhoff and D. C. Sorensen, "P_ARPACK: An Efficient Portable Large Scale Eigenvalue Package for Distributed Memory Parallel Architectures," in *Applied Parallel Computing in Industrial Problems and Optimization*, Jerzy Wasniewski and Jack Dongarra and Kaj Madsen and Dorte Olesen Editors, *Lecture Notes in Computer Science*, Volume 1184, Springer-Verlag (1996) Berlin.

14. G. Evans and R. Greif, "Forced flow near a heated rotating disk: a similarity solution," *Numer. Heat Transfer*, 14, (1988) 373-387.

15. W. G. Breiland and G. H. Evans, "Design and Verification of Nearly Ideal Flow and Heat Transfer in a Rotating Disk Chemical Vapor Deposition Reactor," *J. Electrochem Soc*, 138(6), (1991) 1806-1816.

16. G. Evans and R. Greif, "A numerical model of the flow and heat transfer in a rotating disk chemical vapor deposition reactor," *J. Heat Transfer*, 109, (1987) 928-935.

17. D.I. Fotiadis, S. Kieda and K.F. Jensen, "Transport phenomena in vertical reactors for metalorganic vapor phase epitaxy," *J. Crystal Growth* 102 (1990) 441-470.